

Figure S1. AP4 is expressed in both LZ and DZ GC B cells, related to Figure 1.

(A) Immunofluorescence microscopy showing expression of AP4, c-MYC, AID, and CD23 in human tonsils. LZ and DZ are surrounded by white and yellow dashed lines, respectively. Data are representative of three independent experiments. Scale bar: 100 μ m.

(B) A targeting strategy to generate the AP4-mCherry fusion protein reporter allele.

(C) Southern blot analysis of targeted ES clones. Genomic DNA from WT and one representative targeted ES clone was digested with EcoRI and probed with the 5' probe (left panel) and 3' probe (right panel).

(D and E) Immunoblot analysis showing AP4 and AP4-mCherry expression in GC B cells from *Tfap4^{mCherry/+}* mice eight days after immunization with SRBCs (C), or splenic B cells from the same strain activated with CD40L followed by treatment with cycloheximide (D). Data are representative of two independent experiments.

(F) AP4 and AP4-mCherry protein expression in total, AP4-mCherry⁺, and AP4-mCherry⁻ GC B cells in (D). Data are representative of three independent experiments.

(G) Flow cytometric analysis showing mCherry and GFP expression in GC B cells from the indicated mice eight days after immunization with SRBCs. Data are representative of two independent experiments.

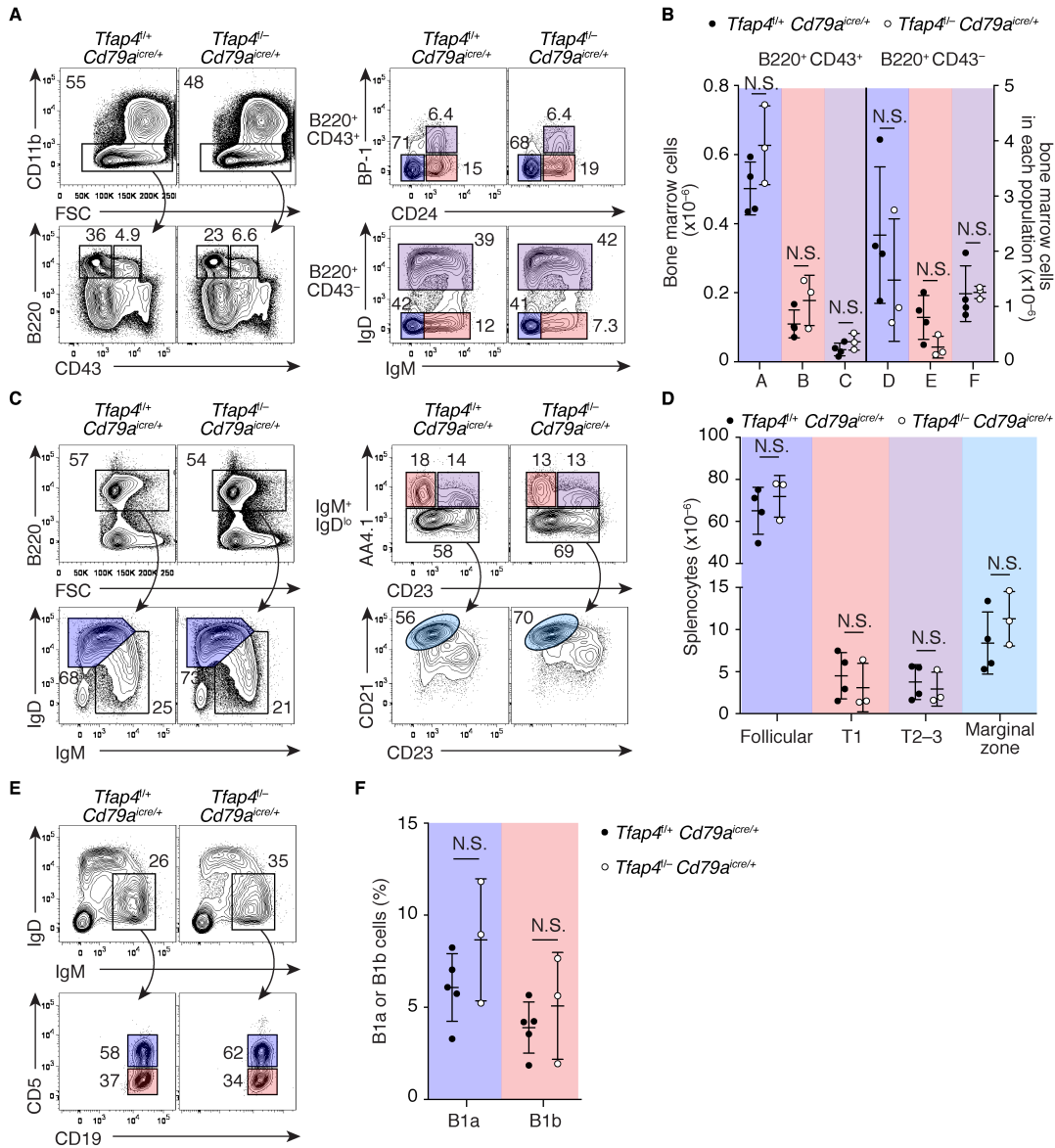


Figure S2. AP4 is dispensable for normal B cell development, related to Figure 2.

(A) Flow cytometric analysis showing expression of CD11b, B220, CD43, BP-1, CD24, IgM and IgD in bone marrow cells from *Tfap4^{fl/-} Cd79a^{icre/+}* (N=4) and control *Tfap4^{fl/+} Cd79a^{icre/+}* mice (N=3).

(B) Absolute numbers of B220⁺CD43⁺ and B220⁺CD43⁻ bone marrow cells per femur in each developmental stage as color-coded in (A).

(C) Expression of B220, IgD, IgM, AA4.1, CD23, and CD21 in splenocytes from *Tfap4^{fl/-} Cd79a^{icre/+}* and control *Tfap4^{fl/+} Cd79a^{icre/+}* mice.

(D) Absolute number of B220⁺ splenocytes in each developmental stage as color-coded in (C).

(E) Expression of IgD, IgM, CD5 and CD19 in cells in peritoneal cavity lavage from *Tfap4^{fl/-} Cd79a^{icre/+}* and control *Tfap4^{fl/+} Cd79a^{icre/+}* mice.

(F) Frequencies of B1a and B1b cells in (E).

Data are pooled from two independent experiments, and shown by means ± SD in (B, D and F). Unpaired Student's *t* test.

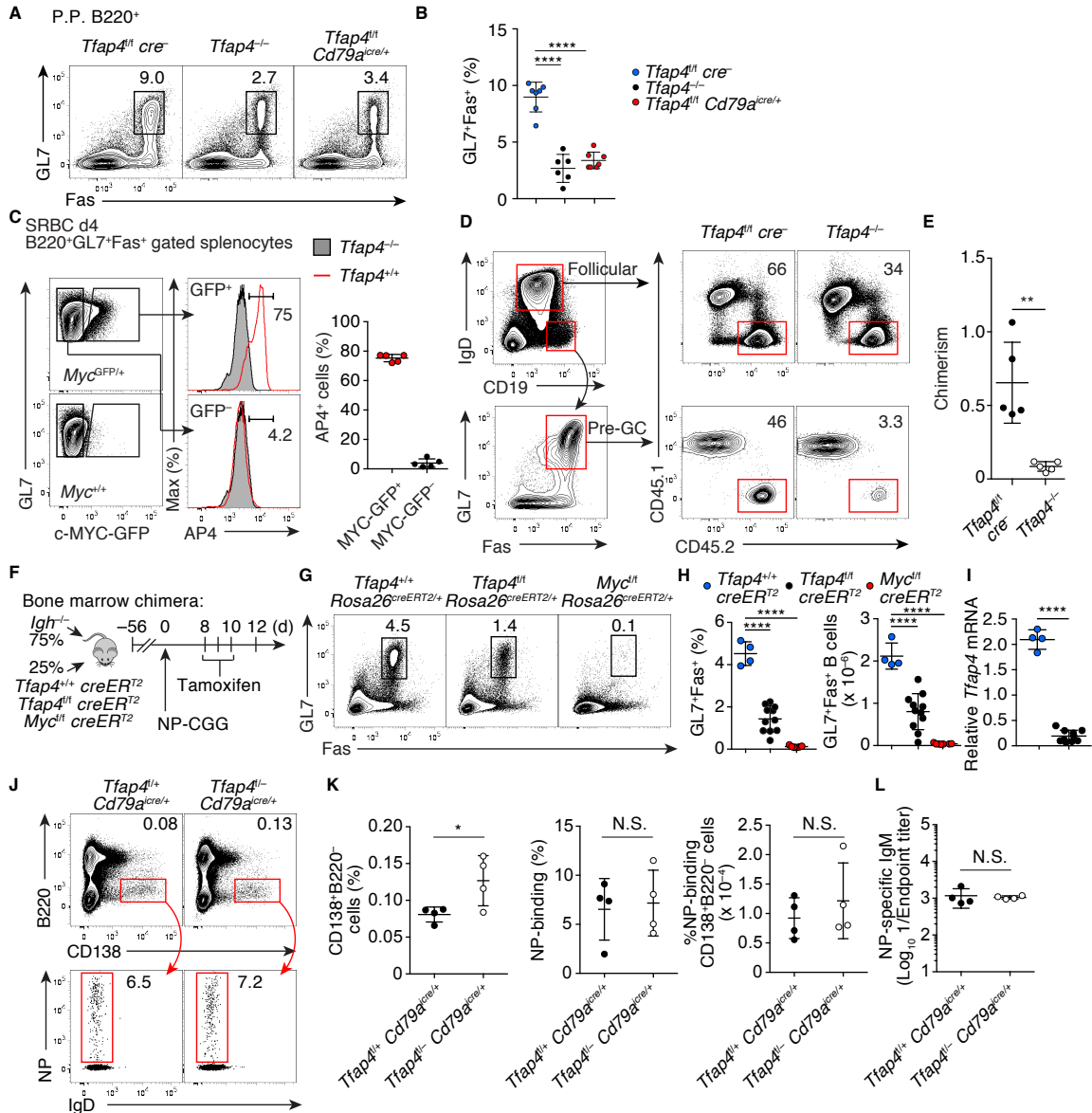


Figure S3. AP4 is required for maximal pre-GC B cell expansion and maintenance of GCs, related to Figure 2.

(A and B) Flow cytometric analysis showing expression of GL7 and Fas on B220⁺-gated cells in Peyer's patches from *Tfap4*^{-/-} (N=6), *Tfap4*^{fl/fl} *Cd79a*^{icre/+} (N=7) and control *Tfap4*^{fl/fl} *cre*⁻ (N=7) mice (A). Statistical analysis of data from two independent experiments is shown in (B).

(C) Intracellular staining for AP4 in c-MYC-GFP⁺ pre-GC B cells four days after immunization with SRBCs (N=5). AP4 staining in *Tfap4*^{-/-} cells is shown as negative control. Data are pooled from two experiments.

(D and E) Flow cytometric and statistical analysis showing the contribution of CD45.2 donor cells to the follicular (IgD⁺CD19⁺) and pre-GC (IgD⁺CD19⁺GL7⁺Fas⁺) B cell compartments in mixed bone marrow chimeras (N=5 per group) five days after NP-CGG immunization. Donor cell contribution to the pre-GC compartment was normalized to that of follicular B cells. Data are pooled from three independent experiments.

(F) Experimental scheme for the generation of mixed bone marrow chimeras used in (G-I). A three to one mixture of bone marrow cells from *Igh*^{-/-} mice and *Tfap4*^{+/+} *Rosa26*^{creERT2/+}, *Tfap4*^{fl/fl} *Rosa26*^{creERT2/+}, or *Myc*^{fl/fl} *Rosa26*^{creERT2/+} mice were transplanted into lethally irradiated B6-CD45.1 hosts. Tamoxifen was

administered on days eight, nine, and ten after immunization with NP-CGG, followed by analysis of GC responses on day 12.

(G) Expression of GL7 and Fas on donor-derived B220⁺ splenocytes from the indicated mixed bone marrow chimeras (N=4-11). Data are representative of four independent experiments.

(H) Frequencies of GL7⁺Fas⁺ in B220⁺ cells (left panel) and absolute numbers of B220⁺GL7⁺Fas⁺ cells in the spleens (right panel) from indicated mixed bone marrow chimeras. Data are pooled from four independent experiments.

(I) *Tfap4* mRNA amounts in B220⁺GL7⁺Fas⁺ splenocytes from the bone marrow chimeras. Data are pooled from two independent experiments.

(J) Expression of B220, CD138, and IgD in splenocytes and intracellular NP-binding in CD138⁺B220⁻ splenocytes from *Tfap4*^{fl/fl} *Cd79a*^{icre/+} (N=4) and control *Tfap4*^{fl/+} *Cd79a*^{icre/+} (N=4) mice seven days after immunization with NP-Ficoll. Data are representative of two independent experiments.

(K) Frequencies and absolute numbers of CD138⁺B220⁻ cells per spleen and the frequency of NP-binding cells in CD138⁺B220⁻ splenocytes in (J). Data are pooled from two independent experiments.

(L) Serum NP-specific IgM titers seven days after NP-Ficoll immunization in (J).

Data are shown by means ± SD. One-way ANOVA for (B and H). Unpaired Student's *t* test for (E, I, K and L).

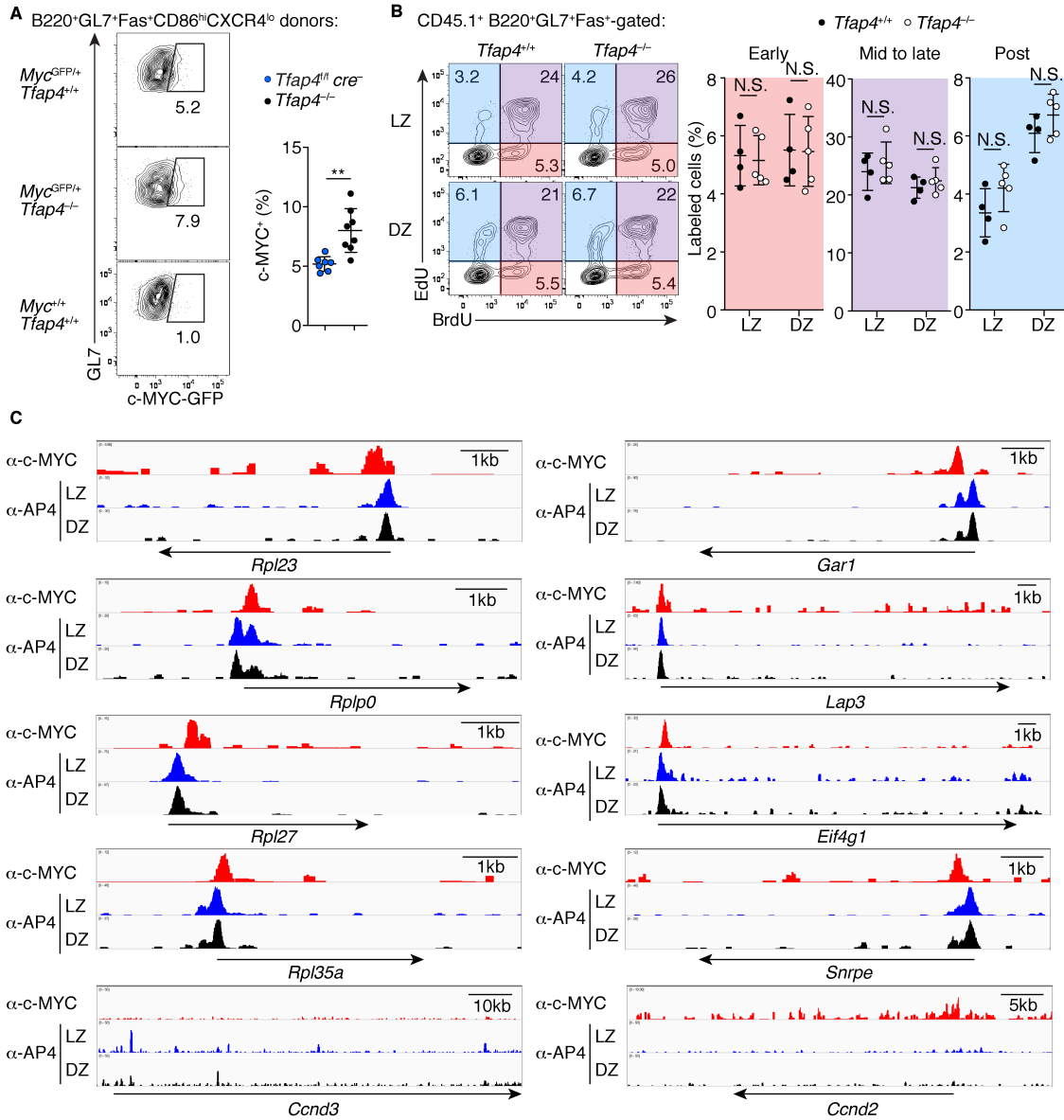


Figure S4. AP4 is dispensable for MYC upregulation in LZ cells following selection, related to Figure 3.

(A) Flow cytometric analysis showing c-MYC-GFP expression in *Tfap4*^{-/-} and control *Tfap4*^{fl/fl cre} LZ GC B cells eight days after NP-CGG immunization (N=7-8 per group). Data are pooled from three independent experiments.

(B) EdU and BrdU incorporation by LZ and DZ GC B cells derived from WT CD45.1 donor cells in mixed bone marrow chimeras (Figure 2D) following sequential pulse labeling with EdU and BrdU as described in Figure 3B. Data are pooled from two independent experiments.

(C) Examples of c-MYC and AP4 binding to genes shown in Figure 4F determined by ChIPseq using sorted LZ or DZ GC B cells or *in vitro* activated B cells.

Data are shown by means \pm SD. Unpaired Student's *t* test.

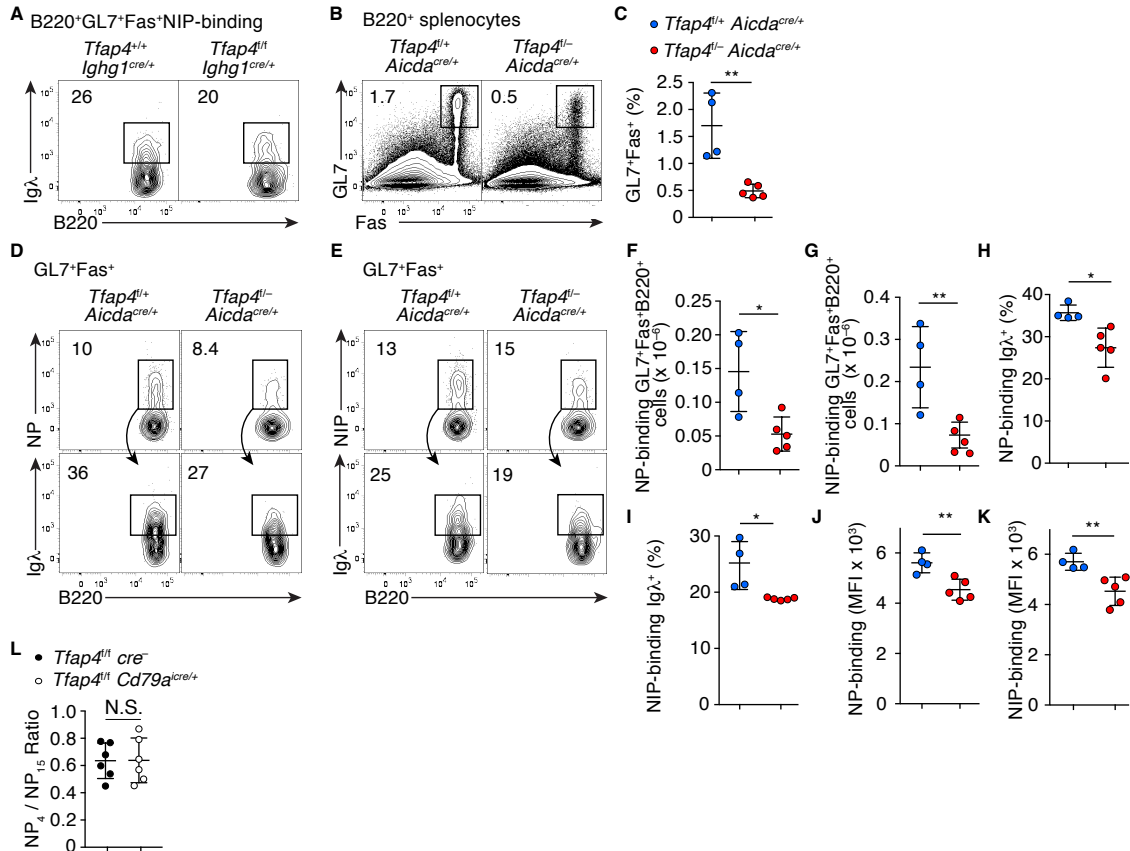


Figure S5. Antibody responses in GC B cell- and activated B cell-specific AP4 conditional knockout mice following immunization with NP-CGG in Alum, related to Figure 5.

(A) Flow cytometric analysis showing Igλ expression in NIP-Allophycocyanin (APC) binding GL7⁺Fas⁺B220⁺ splenocytes from *Tfap4*^{fl/fl} *Ighg1*^{cre/+} (N=5) and control *Tfap4*^{fl/+} *Ighg1*^{cre/+} (N=6) mice ten days after NP-CGG immunization.

(B) Expression of GL7 and Fas in B220⁺ splenocytes from *Tfap4*^{fl/fl} *Aicda*^{cre/+} (N=5) and control *Tfap4*^{fl/+} *Aicda*^{cre/+} (N=4) mice ten days after NP-CGG immunization.

(C) Statistical analysis of frequencies of GL7⁺Fas⁺ cells in B220⁺ splenocytes in (B).

(D and E) NP- and NIP-conjugate APC binding by B220⁺GL7⁺Fas⁺ splenocytes and Igλ expression in NP-APC- or NIP-APC-binding GC B cells in (B).

(F-K) Absolute numbers of and Igλ expression in NP-APC- (F and H) and NIP-APC-binding B220⁺GL7⁺Fas⁺ splenocytes (G and I), as well as NP-APC- (J) and NIP-APC-binding (K) by B220⁺GL7⁺Fas⁺ splenocytes in (B).

(L) Ratio of NP₄- to NP₁₅-specific serum IgG₁ titers from *Tfap4*^{fl/fl} *Cd79a*^{cre/+} (N=6) and control *Tfap4*^{fl/fl} *cre*⁻ (N=6) mice 56 days after NP-CGG immunization.

Data are representative of (A, B, D and E) or pooled from (C and F-L) two independent experiments. Data are shown by means ± SD. Unpaired Student's *t* test.

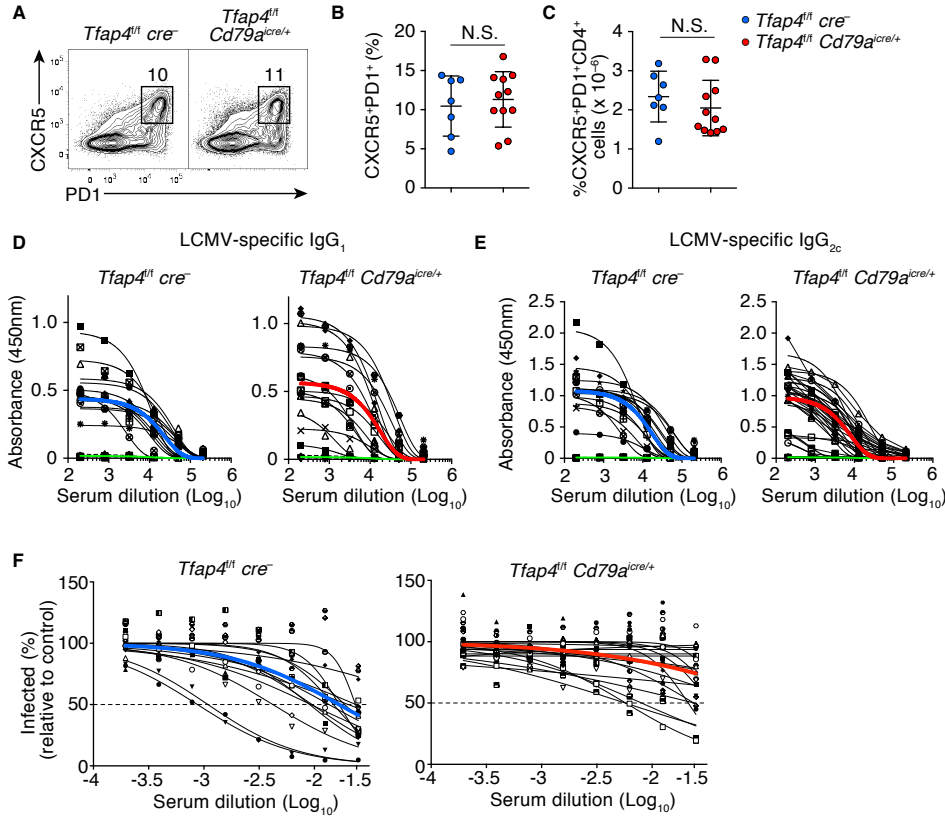


Figure S6. Humoral immune responses to LCMV clone 13 infection in B cell-specific AP4-conditional knockout mice, related to Figure 6.

(A-C) Flow cytometric analysis showing CXCR5 and PD1 expression in CD4⁺ splenocytes from *Tfap4^{fl/fl} Cd79a^{icre/+}* (N=11) and control *Tfap4^{fl/fl} cre⁻* (N=7) mice 30 days after infection with LCMV-c13. Statistical analysis from two independent experiments is shown by means \pm SD in (B and C). Unpaired Student's *t* test.

(D and E) Binding curves showing the reactivity of serum IgG₁ and IgG_{2c} from mice infected with LCMV-c13 to LCMV virion, as determined by ELISA. The thick curves in each group represent the average reactivity to LCMV virion. Green curves, showing reactivity of West Nile Virus vaccine-induced serum IgG to LCMV virion, serve as background controls. Each character symbol represents an individual mouse. Data are pooled from six independent experiments.

(F) Inhibition of LCMV infection of Vero cells by heat-inactivated sera collected from *Tfap4^{fl/fl} Cd79a^{icre/+}* (N=25) and control *Tfap4^{fl/fl} cre⁻* (N=14) mice 80 days after infection. Data are pooled from six independent experiments.

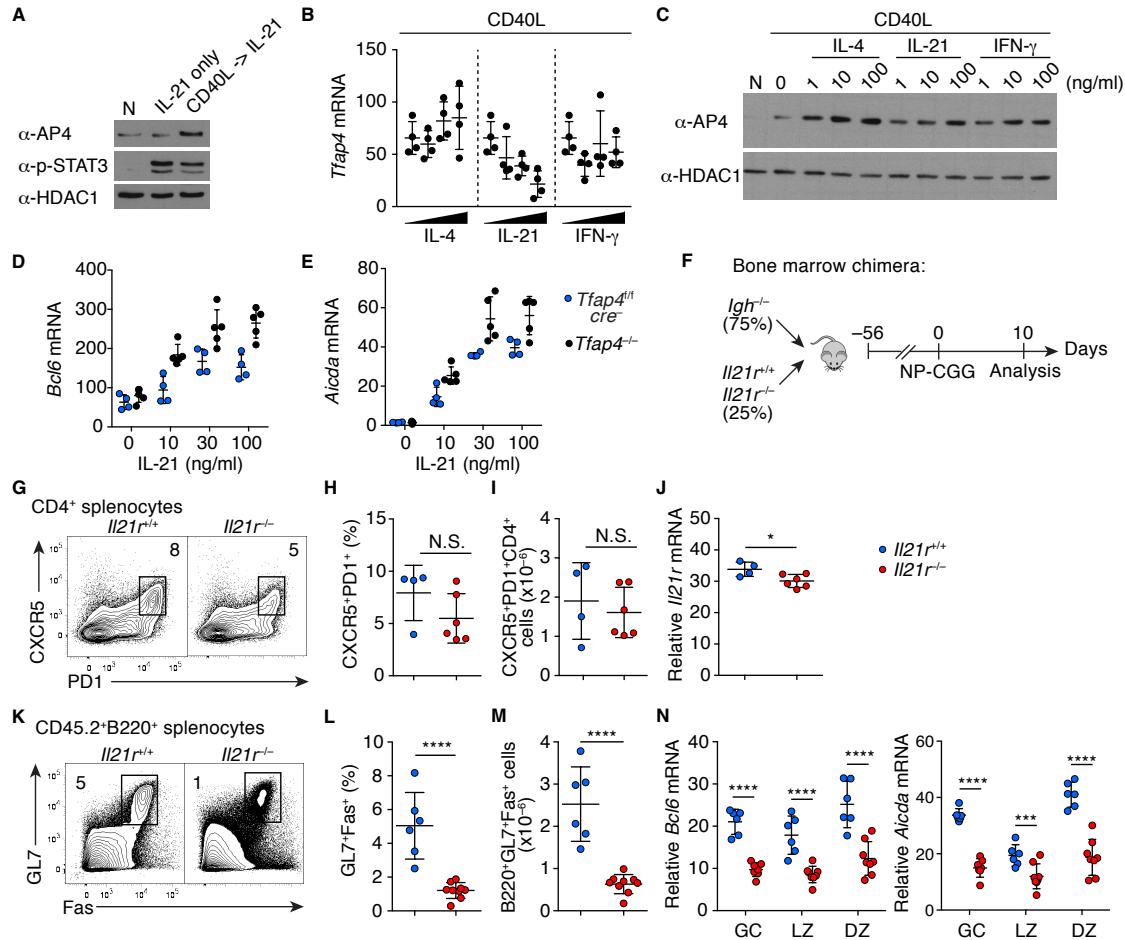


Figure S7. IL-21R signals regulate sustained AP4 expression in GC B cells, related to Figure 7.

(A) Immunoblot analysis showing AP4 and phosphorylated STAT3 protein amounts in naive B cells (N), naive B cells cultured in the presence of IL-21 (IL-21 alone) for 24 hours, and CD40-primed B cells subsequently cultured in the presence of IL-21 (CD40L → IL-21).

(B and C) *Tfap4* mRNA (B) and AP4 protein expression (C) in B cells co-stimulated with CD40L and each cytokine (0, 10, 30, 100 ng/ml). Cell number normalized transcript amounts are shown.

(D and E) *Bcl6* and *Aicda* mRNA expression in *Tfap4*^{+/cre-} (N=5) and control *Tfap4*^{+/+} (N=4) B cells that were sequentially stimulated by CD40 ligation and IL-21. Cell number normalized transcript amounts are shown.

(F) A schematic showing the generation of mixed bone marrow chimeras, in which *Il21r* is deficient in all B cells. A three to one mixture of bone marrow cells from *Igh*^{-/-} mice and *Il21r*^{-/-} or *Il21r*^{+/+} mice were transplanted into lethally irradiated B6-CD45.1 hosts, followed by NP-CGG immunization and analysis of GC responses on day ten.

(G) Flow cytometric analysis showing CXCR5 and PD1 expression in CD4⁺ splenocytes from mixed bone marrow chimeras (N=4-6 per group) in (F).

(H and I) Frequencies (H) and absolute numbers (I) of CXCR5⁺PD1⁺ cells in CD4⁺ cells in (G).

(J) *Il21r* mRNA amounts in CXCR5⁺PD1⁺CD4⁺ splenocytes in (G).

(K) GL7 and Fas expression in donor-derived B220⁺ splenocytes (N=6-9 per group) in (F).

(L and M) Frequencies of GL7⁺Fas⁺ cells in donor-derived B220⁺ splenocytes (L) and absolute numbers of B220⁺GL7⁺Fas⁺ cells per spleen (M) in (K).

(N) *Bcl6* and *Aicda* mRNA amounts in total GC, LZ, and DZ cells in (K).

Data are representative (A, C, G and K) of or pooled (B, D, E, H-J, and L-N) from two independent experiments, and shown by means ± SD. Unpaired Student's *t* test.

Table S1. Lists of genes that were upregulated by T-cell mediated selection and retained at higher levels in AP4⁺ DZ B cells compared to AP4⁻ DZ B cells, related to Figure 4.

Normalized mRNA expression of genes in selected pathways and c-MYC and AP4 occupancy to their genomic loci are shown.

Supplemental Experimental Procedures

Human tissue samples

Tonsils were obtained from routine tonsillectomies performed at the Barnes-Jewish Hospital according to a protocol approved by an Internal Review Committee at Washington University School of Medicine.

Real-time quantitative RT-PCR

RNA was extracted with Trizol (Life Technologies) and was reverse-transcribed with qScript Supermix (Quanta Bio). DyNAmo ColorFlash SYBR green qPCR mix (ThermoFisher) and a LightCycler 480 (Roche) were used for real-time quantitative RT-PCR. Quantities of transcripts were normalized to that of 18S ribosomal RNA unless specified otherwise. For quantification of gene expression normalized to that of 'spiked-in' RNA, 1 ml of ERCC (External RNA Controls Consortium) RNA Spike-In Control Mixes (Ambion) was added at a dilution of 1:10,000 to lysates from 1×10^6 cells prior to RNA extraction. Primers for 18S-rRNA, ERCC-00108, LCMV-NP, *Tfap4*, *Myc* and *Bcl6* were described previously (Chou et al., 2014). The following primers were used:

Aicda, CGTGGTGAAGAGGAGAGATAGTG and CAGTCTGAGATGTAGCGTAGGAA;
Atic, CGTCTCTTGGTTGAGTCTGGT and GGAACCTGTTAGCTCAGACAC;
Cad, GTACGAAGATTGGGAGTTGCAT and CTACGCAGTTCTCATCGACCAT;
Ccnd2, CAGACCTTCATCGCTCTGTG and CGTGAGTGTGTTCACTTCATCA;
Ccnd3, GAAGATGCTGGCATACTGGAT and CCAGGTAGTTCATAGCCAGAGG;
Eif3b, AGGATTTTCGTAGACGACGTGAG and CCGATCTTTGAGTACATCACCA;
Eif4g1, CCTACCGAGTTTGGGACCTAT and ACTAGCAGGAAACTGCTGCAC;
Gar1, TGTCAGAAAACATGAAGGCATC and GCAGCAGCTTGTATGGGTCTAT;
Gart, AGTCTCCTCAGGTCAAGCAAGT and GCACTGTGATCATTGACAGAGAC;
Il21r, TCTGAGAAAGACCCTGAAGGAG and CATGGAGAATCAGCAGGAGTAA
Lap3, AGTGAGAGGTCTCTGGGATCG and TTGTAAATTGTGGCAGGTCATC;
Lsm2, GGAActCAAGAATGACCTGAGC and TGAGGGTATTTCTCAGGGTCTG;
Nme1, CGGTAAAGCCTTGTCTATCTGAA and CTCGAACCGCTTGATGATCT;
Ran, CAGCACAGTACGAGCATGATTT and CCAGCTTCACTTTCTCACAGGT;
Rpl23, CCACAGTTAAGAAAGGCAAACC and CTATGACCCCTGCGTTATCTTC;
Rpl27, TCCAAGATCAAGTCCTTTGTGA and AACAGTCTTGTCCAAGGGGATA;
Rpl35a, AAAGGCCATTGGACACAGAAT and TAGTTTAAATCCGGGATGGGTA;
Rplp0, TGAAGTCCAActACTTTCCTCAA and GTTGTCTGCTCCCAATGAAG;
Rplp2, AACTAGACAGCGTGGGCATC and TTTCCATTCACTCACTGATGA;
Rps10, GGAGGCTGACAGAGACACCTAC and CCTCTAAActGGAActCAGTGG;
Rps16, GTCCCTGGAGATGATCGAG and AGAAGCAAAACAGGCTCCAGTA;
Rps29, ACAGAAATGGCATCAAGAAACC and ATTGTTGGCCTGCATCTTCTT;
Snrpd1, GTGGATGTTGAACCTAAGGTGA and ACCACGTCTCTTCTCTACC;
Snrpe, CAAAAGGTGCAGAAGGTGATG and TTCActTGTTCATACAGCCACA;
Xpot, GCGAGGAAGAGATATTGGAGTG and ATCACAACAGACGTGGCTTCTA.

Flow cytometry

Single-cell suspensions were prepared as described (Chou et al., 2014). The following monoclonal antibodies were used in this study: For sorting of GC B cells, splenocytes were stained with monoclonal antibodies (identified above) before being sorted as B220⁺IgD⁻GL7⁺Fas⁺ cells or B220⁺IgD⁻CD38⁻GL7⁺ on a FACSAria II (BD). For analysis, cells were stained with monoclonal antibodies and were analyzed with an LSRII (BD) or LSR Fortessa (BD), with staining with DAPI (4, 6-diamidino-2-phenylindole; Sigma) or Aqua Live/Dead (L34957, Life Technologies) for the exclusion of dead cells. Intracellular staining of AP4 was performed as previously described (Chou et al., 2014). For cell cycle analysis, mice were injected intravenously 1 mg EdU (Sigma-Aldrich), followed by 2 mg BrdU (Sigma-Aldrich) in PBS one hour later as described (Gitlin et al., 2014). Cells were harvested 30 minutes after BrdU injection and processed using an APC BrdU Flow Kit (BD Pharmingen) and a Click-iT Plus EdU Pacific Blue Flow Cytometry Kit (Invitrogen). BrdU was detected using an AF647-conjugated anti-BrdU antibody (MoBU-1, Invitrogen). Data were analyzed with FlowJo software (TreeStar).

Immunofluorescence microscopy

For the detection of AP4 and c-MYC, tissues were fixed in 4% paraformaldehyde at 4 °C over night before embedding in OCT compound (Sakura Finetek). 8 µm sections were cut on a cryostat (Microm HM 550), fixed in ice-cold acetone, and stained. Sections were mounted with ProLong Gold Antifade Mountant with DAPI (P36935, Life Technologies). For the detection of AID, a Tyramide Signal Amplification System (T30955, Life Technologies) was used. Images were acquired with Zeiss AxioCam MRn microscope equipped with an AX10 camera. Subsequent color balancing, overlaying, and area measurements were performed in an ImageJ software (NIH) and Photoshop (Adobe).

Antibodies

The following antibodies were used in Immunofluorescence microscopy: Alexa Fluor (AF) 488-conjugated anti-IgD (11-26c.2a, Biolegend), AF647-conjugated anti-GL7 (GL-7, Biolegend), anti-Rabbit IgG (4414S, Cell Signaling), biotinylated anti-TCRβ (H57-597, Biolegend), anti-CD35 (8C12, BD), unconjugated anti-AID (MAID-2, eBioscience), anti-human CD23 (NCL-L-CD23-1B12, Leica), anti-c-MYC (ab32072, Abcam), anti-AP4 (Egawa and Littman, 2011). Secondary reagents: Streptavidin-conjugated AF555 (S32355, Life Technologies), biotinylated anti-Rat IgG (6430-08, Southern Biotech), anti-Mouse IgG₁ (A85-1, BD). The following antibodies were used in Flow cytometry: AF488-conjugated anti-CD86 (GL-1, Biolegend), anti-IgD (11-26c.2a, Biolegend), anti-CD45.1 (A20, Biolegend), anti-CD23 (B3B4, Biolegend); FITC-conjugated anti-GL7 (GL-7, Biolegend); PE-conjugated anti-GL7 (GL-7, BD), anti-CD40L (MR1, Biolegend), anti-Igλ (RML-42, Biolegend), anti-CD43 (S7, Biolegend), anti-CD5 (53-7.3, BD), anti-CD93 (AA4.1, Biolegend); PerCP-Cy5.5-conjugated anti-CXCR4 (L276F12, Biolegend), anti-IgG₁ (RMG1-1, Biolegend), anti-IgD (11-26c.2a, Biolegend), anti-B220 (RA3-6B2, Biolegend); PE-Cy7-conjugated anti-Fas (Jo2, BD), anti-B220 (RA3-6B2, Biolegend), anti-CD24 (M1/69, Biolegend); APC-conjugated anti-CD19 (6D5, Biolegend), anti-PD1 (29F.1A12, Biolegend); AF647-conjugated anti-CD45.2 (104, Biolegend), anti-GL7 (GL-7, Biolegend), anti-CD86 (GL-1, Biolegend), anti-IgM (RMM1, Biolegend), anti-CD38 (90, Biolegend); AF700-conjugated anti-CD19 (6D5, Biolegend); APC-Cy7-conjugated anti-CD45.2 (104, Biolegend), anti-B220 (RA3-6B2, Biolegend); Pacific Blue-conjugated anti-IgD (11-26c.2a, Biolegend), anti-B220 (RA3-6B2, Biolegend), anti-CD21/35 (7E9, Biolegend), anti-CD19 (6D5, in house); Brilliant Violet (BV) 510-conjugated anti-B220 (RA3-6B2, Biolegend); BV605-conjugated anti-CD45.1 (A20, Biolegend); and biotinylated anti-CXCR5 (2G8, BD), anti-BP-1 (6C3, Biolegend).

Enzyme-linked immunosorbent assay (ELISA)

Anti-NP antibody titers were assessed using NP₄-BSA (Biosearch), NP₁₅-BSA (Biosearch), biotinylated anti-mouse IgG₁ (A85-1, BD), anti-mouse Igλ (1175-08, Southern Biotech), and horseradish peroxidase-conjugated Streptavidin (554066, BD), which was developed with TMB substrate (S1599, Dako). Anti-LCMV antibody titers were measured as previously described using LCMV virion purified on a 20% sucrose cushion, biotinylated anti-mouse IgG₁ antibody and anti-mouse IgG_{2c} antibody (1077-08, SouthernBiotech) (Ahmed et al., 1984; Kunz et al., 2003). Endpoint titers were calculated by a one-phase exponential decay curve using a Prism 6 software (Graphpad) (Purtha et al., 2011).

Immunoglobulin sequence analysis

An intronic sequence 3' to the J_{H4} exon of *Igh* and the V_{H186.2} sequences were PCR amplified from genomic DNA extracted from 3,000-5,000 GC B cells using Phusion HF (Thermo) and oligonucleotide primers described previously (Gitlin et al., 2014). PCR products were gel extracted, cloned into a pCR2.1-TOPO vector (Life Technologies), and sequenced. Obtained J_{H4} intronic sequences were aligned to the mm9 assembly of the mouse genomic sequence. V_{H186.2} sequences were analyzed with ImMunoGeneTics (IMGT) V-QUEST (<http://www.imgt.org/>) (Brochet et al., 2008; Lefranc et al., 2009). Mutation frequencies in the J_{H4} intronic region were calculated by dividing the total number of mutations from all clones with the total number of base pairs analyzed for each group. For mutation analysis of the immunoglobulin heavy chain gene, 5,000-20,000 GC B cells were purified from spleens 30 days after LCMV clone 13-infection. Total RNA was extracted using TRIzol and cDNA was synthesized using the SuperScript III first-strand synthesis system (Invitrogen) with a Cg2c (Outer) primer (Tiller et al., 2009), followed by a semi-nested PCR using Phusion HF. An adaptor-tagged promiscuous V_H (MsVHE) primer (5'-TCTTTCCCTACACGACGCTCTTCCGATCTGGGAATTCGAGGTGCAGCTGCAGGAGTCTGG-3') and an adaptor-tagged Cg2c primer (5'-GTGACTGGAGTTCAGACGTGTGCTCTTCCGAGCTCAGG

GAAATAACCCTTGAC-3') were used for the first round PCR (Tiller et al., 2009). The following primers were used for the second round PCR: 5'-AATGATACGGCGACCACCGAGATCTACACTCTTTCC CTACACGAC-3' and 5'-CAAGCAGAAGACGGCATAACGAGATNNNNNNNGTGACTGGAGTTCA GACG-3' (NNNNNNN: sample-specific bar codes). The PCR products were quantitated using Qubit (Invitrogen) and pooled in equimolar ratios for paired-end 2x250 bp sequencing on an Illumina MiSeq DNA sequencer. To determine the mutation frequency in the VDJ coding regions, only reads longer than 400 bp and with an average qscore > 30 were analyzed with IMGT HighV-QUEST (Brochet et al., 2008; Lefranc et al., 2009). All sequences with >90% identity to the reference sequences from the IMGT database were used for mutation analysis. Only mutations with a qscore > 22 were counted.

Chromatin Immunoprecipitation Assay

For anti-c-MYC ChIP, splenic naive B cells, purified with anti-CD19 microbeads (Miltenyi), were activated with 10 mg/ml of anti-IgM (115-005-020, Jackson ImmunoResearch) for two days, and further cultured on CD40L-expressing NIH 3T3 feeder cells for 24 hours. For anti-AP4 ChIP, splenic LZ and DZ GC B cells eight days after immunization with SRBCs were purified by sorting on a FACS AriaII. Anti-c-MYC, anti-AP4 and anti-H3K27ac (ab4729, Abcam) ChIPs were performed as previously described (Chou et al., 2014). Sequence tags were mapped onto the NCBI37 mm9 with Bowtie2 (Langmead and Salzberg, 2012). The Homer software package (Heinz et al., 2010) was used for peak calling with a Poisson *P*-value cutoff of 1×10^{-40} for AP4 and 1×10^{-6} for c-MYC for extraction of the 4758 and 4046 peaks with the highest statistical significance, respectively.

RNAseq Analysis

Total RNA was purified from 3,000 - 10,000 sorted c-MYC⁻AP4⁻ LZ, c-MYC⁺AP4⁺ LZ, AP4⁺ DZ, and AP4⁻ DZ GC cells from AP4-mCherry/c-MYC-GFP reporter mice eight days after immunization with SRBCs (Figure 4A) using a Nucleospin RNA XS extraction kit (Macherey-Nagel) according to the manufacturer's instructions. The purified RNA was reverse-transcribed and amplified using a SMART-Seq v4 Ultra Low Input RNA Kit (Clontech), followed by library construction using a Nextera DNA Library Prep Kit (Illumina). High throughput sequencing was performed using a HiSeq 2500 sequencer (Illumina) with a 50 bp single read option. Sequence tags were mapped onto the NCBI37 mm9 with TopHat (Trapnell et al., 2009), followed by transcript assembly and RPKM estimation using Cufflinks (Roberts et al., 2011a; Roberts et al., 2011b; Trapnell et al., 2013; Trapnell et al., 2010) on the Galaxy platform (<https://usegalaxy.org/>). Analysis was done with three biological replicates and genes upregulated in c-MYC⁺AP4⁺ relative to c-MYC⁻AP4⁻ LZ cells by more than 1.8-fold with a Student's *t*-test *P*-value less than 0.1 were analyzed by hierarchical clustering using Euclidean distance matrix with centroid linkage. Pathway analysis was performed using a web-based gene set analysis toolkit (<http://bioinfo.vanderbilt.edu/webgestalt/>).

Immunoblot analysis

Whole cell extracts were prepared by lysis of cells in Laemmli buffer containing 1% SDS and 2% 2-mercaptoethanol. Lysates from equal numbers of cells were separated by 8% or 10% SDS PAGE and transferred to PVDF membranes (Roche). Membranes were incubated with primary antibodies (identified below), followed by detection with horseradish peroxidase-conjugated species-specific antibody to immunoglobulin light chain (115-035-174, 211-032-171; Jackson ImmunoResearch) and a Luminata HRP substrate (Millipore). Anti-AP4 was described (Chou et al., 2014). The following antibodies were purchased: anti-Puromycin (MABE343; Millipore), anti-c-MYC (9402S; Cell Signaling), anti-phospho-STAT3 (Tyr705) (9145; Cell Signaling) and anti-BCL6 (4242S, Cell Signaling). Anti-HDAC1 (ab7028; Abcam) was used as loading controls.

References for Supplemental Experimental Procedures

- Ahmed, R., Salmi, A., Butler, L.D., Chiller, J.M., and Oldstone, M.B. (1984). Selection of genetic variants of lymphocytic choriomeningitis virus in spleens of persistently infected mice. Role in suppression of cytotoxic T lymphocyte response and viral persistence. *J Exp Med* *160*, 521-540.
- Brochet, X., Lefranc, M.P., and Giudicelli, V. (2008). IMGT/V-QUEST: the highly customized and integrated system for IG and TR standardized V-J and V-D-J sequence analysis. *Nucleic acids research* *36*, W503-508.
- Chou, C., Pinto, A.K., Curtis, J.D., Persaud, S.P., Cella, M., Lin, C.C., Edelson, B.T., Allen, P.M., Colonna, M., Pearce, E.L., *et al.* (2014). c-Myc-induced transcription factor AP4 is required for host protection mediated by CD8+ T cells. *Nat Immunol* *15*, 884-893.
- Egawa, T., and Littman, D.R. (2011). Transcription factor AP4 modulates reversible and epigenetic silencing of the Cd4 gene. *Proc Natl Acad Sci U S A* *108*, 14873-14878.
- Gitlin, A.D., Shulman, Z., and Nussenzweig, M.C. (2014). Clonal selection in the germinal centre by regulated proliferation and hypermutation. *Nature* *509*, 637-640.
- Heinz, S., Benner, C., Spann, N., Bertolino, E., Lin, Y.C., Laslo, P., Cheng, J.X., Murre, C., Singh, H., and Glass, C.K. (2010). Simple combinations of lineage-determining transcription factors prime cis-regulatory elements required for macrophage and B cell identities. *Molecular cell* *38*, 576-589.
- Kunz, S., Edelmann, K.H., de la Torre, J.C., Gorney, R., and Oldstone, M.B. (2003). Mechanisms for lymphocytic choriomeningitis virus glycoprotein cleavage, transport, and incorporation into virions. *Virology* *314*, 168-178.
- Langmead, B., and Salzberg, S.L. (2012). Fast gapped-read alignment with Bowtie 2. *Nat Methods* *9*, 357-359.
- Lefranc, M.P., Giudicelli, V., Ginestoux, C., Jabado-Michaloud, J., Folch, G., Bellahcene, F., Wu, Y., Gemrot, E., Brochet, X., Lane, J., *et al.* (2009). IMGT, the international ImMunoGeneTics information system. *Nucleic acids research* *37*, D1006-1012.
- Purtha, W.E., Tedder, T.F., Johnson, S., Bhattacharya, D., and Diamond, M.S. (2011). Memory B cells, but not long-lived plasma cells, possess antigen specificities for viral escape mutants. *J Exp Med* *208*, 2599-2606.
- Roberts, A., Pimentel, H., Trapnell, C., and Pachter, L. (2011a). Identification of novel transcripts in annotated genomes using RNA-Seq. *Bioinformatics* *27*, 2325-2329.
- Roberts, A., Trapnell, C., Donaghey, J., Rinn, J.L., and Pachter, L. (2011b). Improving RNA-Seq expression estimates by correcting for fragment bias. *Genome Biol* *12*, R22.
- Tiller, T., Busse, C.E., and Wardemann, H. (2009). Cloning and expression of murine Ig genes from single B cells. *J Immunol Methods* *350*, 183-193.
- Trapnell, C., Hendrickson, D.G., Sauvageau, M., Goff, L., Rinn, J.L., and Pachter, L. (2013). Differential analysis of gene regulation at transcript resolution with RNA-seq. *Nat Biotechnol* *31*, 46-53.
- Trapnell, C., Pachter, L., and Salzberg, S.L. (2009). TopHat: discovering splice junctions with RNA-Seq. *Bioinformatics* *25*, 1105-1111.
- Trapnell, C., Williams, B.A., Pertea, G., Mortazavi, A., Kwan, G., van Baren, M.J., Salzberg, S.L., Wold, B.J., and Pachter, L. (2010). Transcript assembly and quantification by RNA-Seq reveals unannotated transcripts and isoform switching during cell differentiation. *Nat Biotechnol* *28*, 511-515.